

Biophysical Journal, Volume 97

**Supporting Material**

**Simulations studies of Stratum Corneum lipid mixtures**

Das Chimnay, Massimo Noro, and Peter Olmsted

## Supplementary material

In the supplementary material we present some additional results from the simulations presented in the main paper. Also we provide results from some additional simulations to address the effects of long range electrostatics, equilibration, run times and system size.

### Temperature dependence of structural quantities:

Structural quantities for the SC lipid bilayers were found to vary smoothly with temperature. We have shown the temperature dependence of CER bilayer in Figs. 6 and 7 of the paper. In Fig. S1 we show the area compressibility and bilayer thickness of 2:2:1 system as a function of temperature.

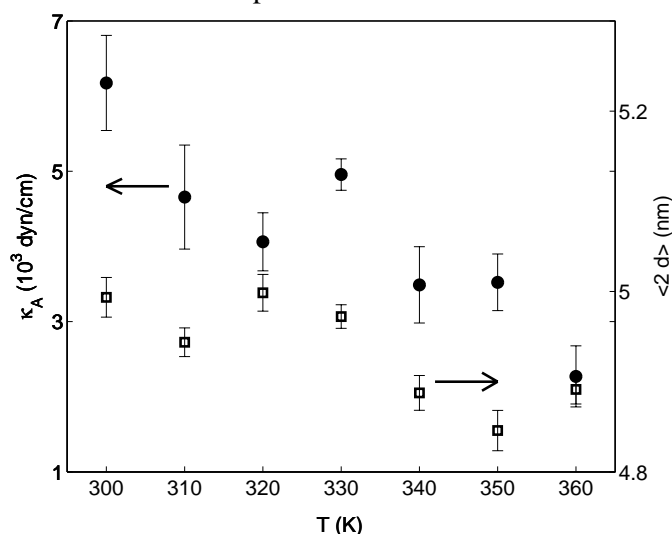


**Fig. S1:** Area compressibility (circles, left y-axis) and average density (squares, right y-axis) of a mixed system, CER:CHOL:FFA=2:2:1, as a function of temperature.

### Orientalional order of fatty acid tails:

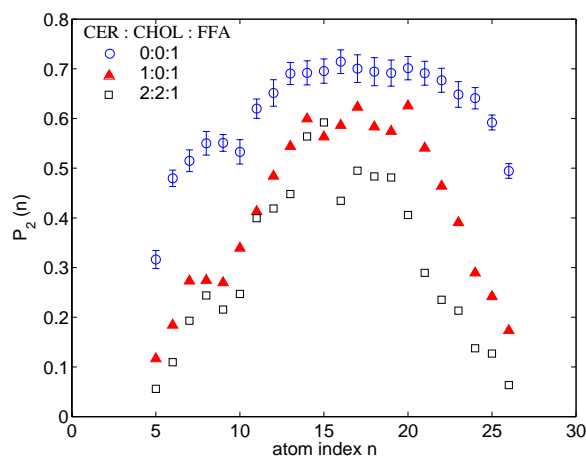


**Fig. S2:** Local tail order parameter ( $P_2$ ) as a function of atom index  $n$  on a FFA molecule (see Fig.1) for various compositions at 340 K.

In the main text we only considered the orientational ordering  $P_2$  of the CER tails (Fig. 12). Similar analyses were also done with FFA (Fig. S2). In the presence of CER or CHOL molecules,  $P_2$  for the fatty acid atoms behave similar to that of the long tail of CER molecules.

### Numerical data for the structural quantities:

In Table S1, we present the numerical values of the structural quantities measured and presented as figures in the main text.

composition (molar ratio)	$2d$ (nm)	$\bar{\rho}_L$ (g/cc)	$\rho_L^{mid}$ (g/cc)	$\lambda_{ov}$ (nm)	$\kappa_A$ ( $10^3$ ) (dyn/cm)	$\kappa$ ( $10^{-11}$ ) (erg)	$\bar{\epsilon}_P$ (bar)
1:0:0	5.66	0.95	0.66	1.30	4.9	6.6	660
0:1:0	3.16	1.03	0.91	–	4.7	1.9	870
0:0:1	6.33	0.92	0.51	–	1.5	2.6	580
7:1:0	5.56	0.95	0.68	0.93	6.3	8.1	580
3:1:0	5.29	0.95	0.68	1.16	4.4	5.2	460
2:1:0	5.16	0.95	0.67	1.42	5.5	6.1	500
1:1:0	4.75	0.96	0.73	1.87	4.9	4.6	400
7:0:1	5.73	0.95	0.63	0.90	4.4	6.0	640
3:0:1	5.81	0.95	0.64	1.10	3.7	5.2	620
2:0:1	5.88	0.95	0.61	0.90	4.2	6.0	570
1:0:1	5.91	0.94	0.60	1.42	2.4	3.5	550
1:1:1	5.17	0.94	0.72	2.20	4.9	5.5	350
1:2:1	4.99	0.96	0.80	2.52	4.5	4.7	390
2:1:1	5.82	0.93	0.77	3.33	2.3	3.3	350
5:5:1	4.94	0.95	0.74	1.48	5.2	5.3	480
2:2:1	4.89	0.94	0.69	2.50	3.9	3.9	360

**Table S1:** Structural properties of SC lipid bilayers for different ratios of CER:CHOL:FFA molecules at 340K.

### Simulations with larger system size and run time:

To explore the dependence of measured quantities on system size and run times, we have carried out some additional simulations on pure CER bilayers and bilayers with 2:2:1 composition ratio of CER, CHOL, FFA. These simulations use much larger number of lipid molecules and much longer run times than the simulations reported in the paper.

Composition	Number of molecules				Run time (ns)	
	CER	CHOL	FFA	SOL	Cutoff	PME
2:2:1 (340K)	56	56	32	5250	100	100
	224	224	128	21000	70	40
	504	504	288	47250	50	16
1:0:0 (300K)	128	--	--	5250	30	30
	512	--	--	21000	30	16
	1152	--	--	47250	20	10

**Table. S2:** Number of molecules and simulation times used for the supplementary material.

To get the initial configuration for a larger system, we use the already equilibrated configuration from the simulations presented in the paper and replicate it in the x and y directions. Table S2 shows the number of molecules and simulation time scales used for these studies. To reduce disk space requirements, in most cases of these set of simulations, we save configurations only at intervals of 0.2 ns (as opposed to 0.5 ps in the main paper). Thus we expect larger statistical errors in the data reported in this supplementary material as compared to the main paper.

## Equilibra

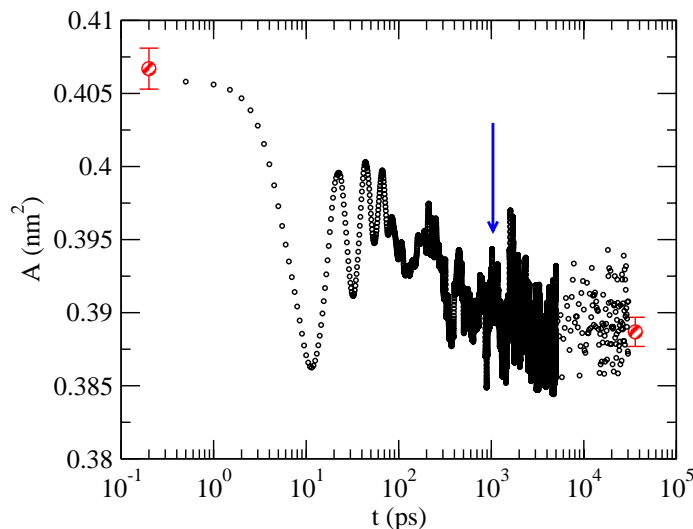


**Fig. S3:** Equilibration of area/lipid for a CER bilayer after a sudden change in thermostat temperature from 360 K to 300 K. The big circles with error-bars are the values obtained from different runs at 360K and 300K.

To probe the typical time it takes for the system to adapt the equilibrium conformation for a given temperature, we used an equilibrated configuration of 128 CER lipids (1:0:0 composition) at 360 K and monitored the instantaneous area/lipid as a function of time (small black circles in Fig. S3) after abruptly changing the desired thermostat temperature to 300 K. We also show the area/lipid calculated from separate runs at 360 K and at 300 K as shaded big circles with error bars at the two extreme ends of the data. As can be seen from the plot, the area/lipid adapts to the new temperature with a time scale of around 1 ns (position of the arrow). In the paper we use equilibration times of 10 ns for each 10K temperature shift – which gives ample time for the molecules to reorganize themselves into the equilibrium conformation corresponding to the set temperature.

Once the average values no longer show a systematic drift in time, one can evaluate the mean values and error estimates on the mean value, provided there is enough *uncorrelated* data. Fig. S4 shows the autocorrelation function of area fluctuation in a simulation of 128 CER molecules at 300K. The correlation decays within a time scale of about 100 ps. Thus the results reported in the paper, which use data from 10 ns runs, have sufficient number of uncorrelated data to give robust estimates of the mean and errors in the mean.

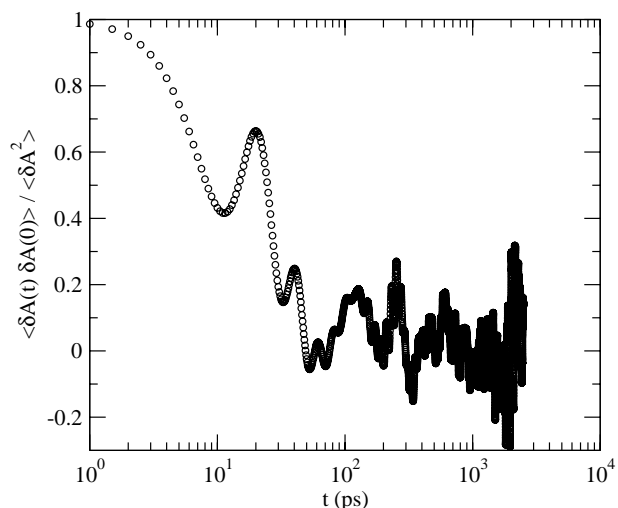


**Fig. S4:** Decay of auto-correlation in area fluctuation for ceramide bilayer at 300K.

### Dynamics of lipid molecules

The lipid compositions probed in this work remain in a *gel* phase for all temperature ranges considered. By the word *gel*, we mean a soft glassy state, where there is a large separation of atomic time scale (fs) and center of mass hopping (ns). At long times, the system is ergodic and acquires a hopping dominated diffusive dynamics.

Lipids in pure CER bilayers acquire a close packed structure in the x-y plane. However, the chains remain highly mobile in the z-direction, undergoing a slithering movement, with the longer hydrocarbon tail repeatedly undergoing extended and folded conformation (Fig. 2c). In most of the snapshots the short tail remains straight, while the long tail often develops a large kink, sometimes pulling the atoms into a large loop close to the head group. The close-packing of the CH<sub>2</sub> groups in the x-y plane allows only correlated hopping, except at the places with defects (mainly 5 and 7 co-ordinated arrangements). With time, the two leaflets undergo a rocking movement, with sudden jumps changing the registry between the two leaflets.

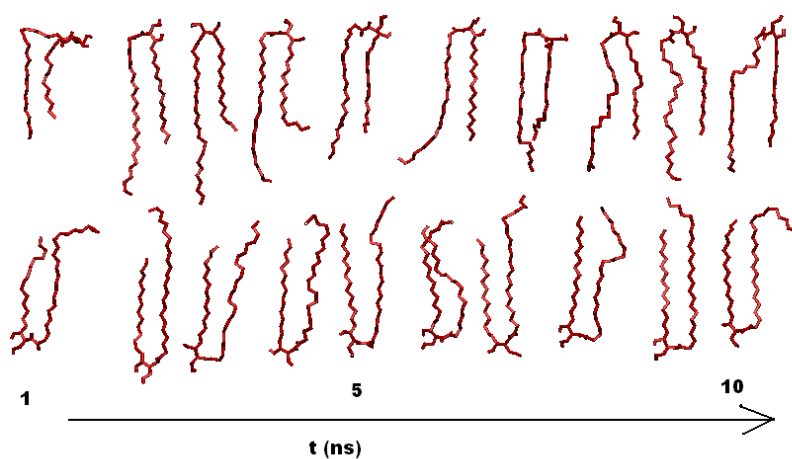


**Fig. 2c:** Slithering motion of Ceramide tails in two selected molecules.

Cholesterol disrupts the in-plane registry. The lipid molecules still spend a long time in cages defined by their neighbors. But the occasional jumps are no longer correlated for bilayers containing cholesterol molecules. Fig. S5 shows 70-ns trajectories of the centers of mass of the lipids in one leaflet of 2:2:1 composition ratio of CER:CHOL:FA (576 lipid system) projected on the x-y plane. The red, green and blue traces respectively refer to the CER, CHOL and FA molecules. Both CHOL and FA molecules typically cover distances larger than inter-lipid separation in this time-scale. The molecular diffusion is anisotropic, as determined by the in-plane order of the hydrocarbon tails.

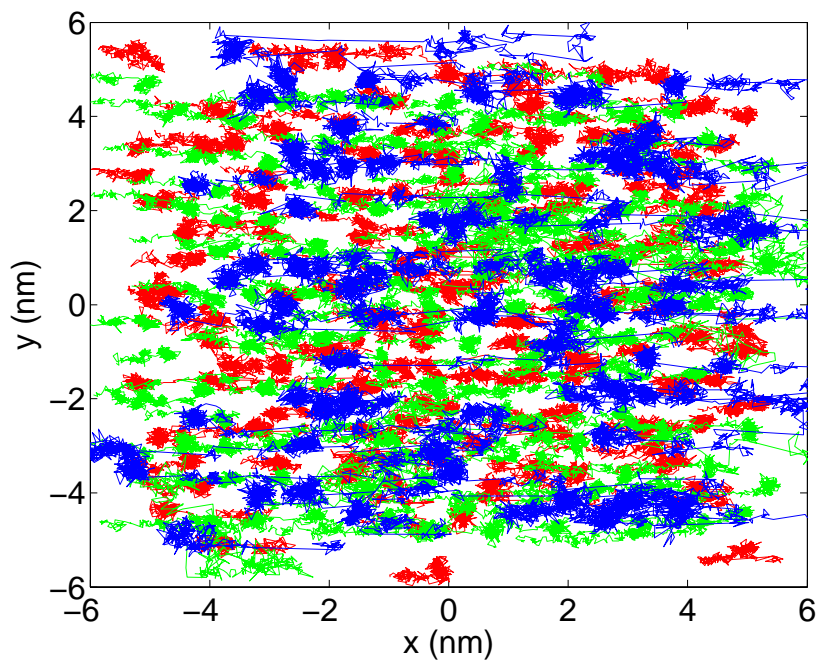


**Fig. S5:** Trajectories of center of masses of CER (red), CHOL (green) and FFA (blue) molecules from a single leaflet of 2:2:1 bilayer covering 70 ns at 340K.

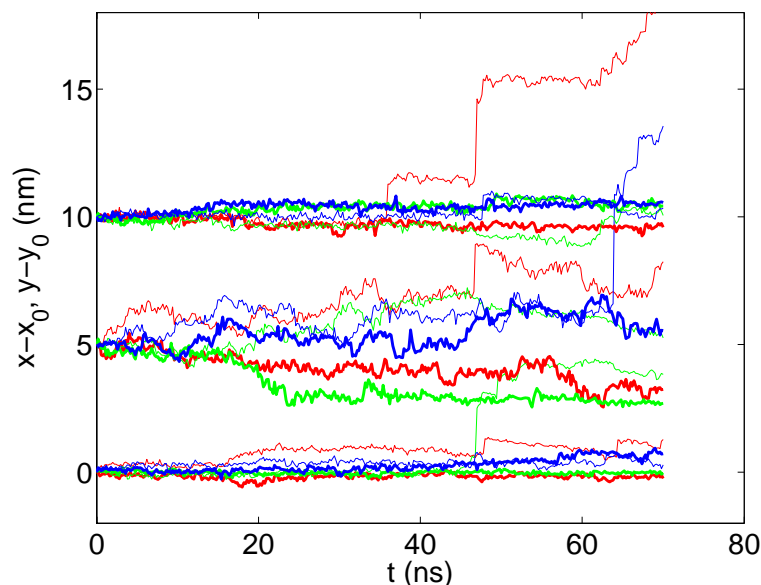


**Fig. S6:** Time trace of projected displacements along the x direction (thin lines) and the y direction (thick lines) for center of masses of three molecules each of CER, CHOL (initial displacements are shifted by 5 nm) and FA (initial displacements are shifted by 10 nm).

Fig. S6 shows the time trace of the displacement components of three molecules each from CER, CHOL and FFA. The FA molecules are especially mobile, with one of the molecules moving by about 3 nm along the x direction within 2 ns. Consistent with the hopping-limited dynamics, displacements are localized in time: e.g. the large steps of order 0.5 nm occurring over a ns timescale in Fig. S6.

### Effect of long range electrostatics and system size

As mentioned in the main paper, the dominant electrostatic interactions in the lipids considered in this work are dipole-dipole interactions, with typical dipole moments smaller than those of water molecules. In simulations of phospholipid bilayers (where the head group ionizes, giving rise to dipole moments which are about 15 times larger than the typical dipole moments involved in the current simulations), exclusion of the long range electrostatics, especially for small system sizes, cause serious artefacts (Wohlert and Edholm, *Biophys. J.*, **87**, 2433--2445, 2004). We can estimate the relevance of long range electrostatics by comparing the dipole moments involved in ceramides with the literature results on phospholipid simulations. In the paper, we argued that such a comparison shows that the effect of long range electrostatics should be negligible for our system.

In Table S3, we report the energies (normalized by the number of lipid molecules in the system) for 2:2:1 system calculated separately with group based cut-off and particle mesh Ewald summation (PME). In simulation with PME, the grid spacing was chosen to be 0.1 nm and fourth order polynomial interpolation was used. The simulation time scales are in Table. S2.

Number of lipids		Coulomb (SR)*	Coulomb (LR)*	Total energy*	$\kappa_A$ ( $10^3$ dyne/s)	2 d (nm)
144	cut-off	-1.7675	----	-1.1310	2.6 (2)	4.90 (2)
	PME	-1.6363	-0.1101	-1.1114	2.0 (3)	4.95 (2)
576	cut-off	-1.7676	----	-1.1308	2.5 (5)	4.97 (2)
	PME	-1.6364	-0.1101	-1.1105	3.6 (3)	4.91 (2)
1296	cut-off	-1.7676	----	-1.1302	2.3 (5)	4.93 (2)
	PME	-1.6364	-0.1102	-1.1104	2.9 (4)	4.90 (1)

**Table. S3:** Short range (SR) and long range (LR) electrostatic energies, total energy, area compressibility ( $\kappa_A$ ) and bilayer thickness (2d) for systems containing 2:2:1 molar ratio of CER2, CHOL and FFA at 340K. Statistical errors of the mean values are indicated in the brackets as the uncertainty on the last digit. (\* Energies are in MJ/mol and are normalized by the number of lipid molecules in the system.)

The two important observations from the energy values are that (i) the difference between the group based cut-off and PME schemes in the total energy is about 2% and (ii) the normalized energies are independent of the system sizes. Both of these two observations show that the interactions with the periodic images do not contribute significantly in the electrostatic energy. Table. S3 also shows the area compressibility and the average bilayer thickness calculated from these simulations. The effect of the system size and handling of electrostatics do not affect the values significantly.

Table S4 shows the effect of system size and method of calculating electrostatic interaction for pure CER bilayers at 300K. The conclusions about insensitivity of the results on both the system size and the long range electrostatic interaction in the case of 2:2:1 lipid mixture remains equally valid for the case of CER bilayers.

Number of lipids		Coulomb (SR)*	Coulomb (LR)*	Total energy*	$\kappa_A$ ( $10^3$ dyne/s)	2 d (nm)
128	cut-off	-2.2045	----	-1.5516	7.0 (6)	5.67 (1)
	PME	-1.9974	-0.1755	-1.5272	6.1 (6)	5.68 (1)
512	cut-off	-2.1996	----	-1.5520	6.2 (9)	5.70 (1)
	PME	-1.9973	-0.1754	-1.5269	7.4 (9)	5.70 (1)
1152	cut-off	-2.1994	----	-1.5516	5.8 (7)	5.72 (1)
	PME	-1.9946	-0.1753	-1.5245	7.4 (9)	5.72 (1)

**Table. S4:** Short range (SR) and long range (LR) electrostatic energies, total energy, area compressibility ( $\kappa_A$ ) and bilayer thickness (2d) for pure CER bilayers at 300K. (\*Energies are in MJ/mol and are normalized by the number of lipid molecules in the system.)

For the smallest system sizes used in this study, typical CPU requirements for PME based calculations are more than twice as compared to the CPU requirement for group-based cut-off. Hence, for the simulation results presented in the main paper, we confine ourselves to group-based cut-off scheme only.